

MULTIMODAL LLM-GUIDED QUERY OPTIMIZATION FOR VISUAL-LANGUAGE RETRIEVAL

Anonymous authors

Paper under double-blind review

ABSTRACT

Vision-language retrieval (VLR), involving the use of text (or images) as queries to retrieve corresponding images (or text), has been widely used in multimedia and computer vision tasks. However, ambiguous or complex concepts contained in queries often confuse retrievers, making it difficult to effectively align these concepts with visual content, thereby limiting their performance. Existing query optimization methods neglect the feedback of retrievers' preferences, thus resulting in sub-optimal performance. Inspired by the powerful ability of Multimodal Large Language Models (MLLMs), we propose a Multimodal LLM-Guided Query Rewriter (MGQRe) for query optimization. Specifically, MGQRe first utilizes MLLM to explore the retriever's weakness and perform targeted iterative optimizations to capture the retriever's expressive preferences. Subsequently, we develop a trainable rewriter that learns this preference knowledge through a three-step tuning strategy: supervised fine-tuning, preference learning, and reinforcement learning. This ensures that the queries generated by the rewriter align with the retriever's preferences, thereby enhancing the retriever's performance. Extensive VLR benchmark experiments have demonstrated the superiority of MGQRe, as well as its generalizability and transferability. This work showcases the potential of using advanced language models to overcome the inherent limitations in current VLR technology.

1 INTRODUCTION

Vision-language retrieval (VLR), which involves the using of text/image as queries to retrieve corresponding image/text, has garnered significant attention from both academia and industry. Existing methods (Radford et al., 2021; Li et al., 2022; Yu et al., 2022) mainly focus on how to align text and image modalities within a shared semantic space.

Despite the progress in VLR, existing methods still face challenges on complex or ambiguous concepts in queries, due to the heterogeneity of data. For example, as illustrated in Fig 1, the retriever failed to perceive the visual features associated with the term "anticipate", thus resulting in irrelevant images. This confusion often leads to the retriever's inability to accurately align these concepts with corresponding visual features, which typically limits the performance of multimodal retrieval. To alleviate such issues, it is expected to utilize a rewriter to optimise complex concepts in the query. However, traditional rewriting methods struggle to effectively adapt queries based on the retriever's preferences, leading to suboptimal retrieval results (see Fig 1). Ensuring that the rewriter generates queries that align with the retriever's understanding preferences poses a significant challenge. Typically, exploring the retriever's preferences requires extensive human analysis and repetitive iterations to adapt queries, which is both time-consuming and costly. Multimodal large language models (MLLMs) (Wang et al., 2024; Jin et al., 2024) have demonstrated impressive analytical capabilities for addressing complex issues. Therefore, employing MLLMs as agents to capture the retriever's fine-grained preferences offers an efficient and practical solution.

Based on these observations, we propose the MLLMs-Guided Query Rewriter (MGQRe) for VLR. First, MLLMs capture the fine-grained preferences of the retriever, and a rewriter is then developed to learn preference knowledge. Specifically, we employ MLLMs as agents that mine the retriever's preferences. Based on the feedback from the retriever on the query, MLLMs continuously explore the retriever's weaknesses and iteratively optimize the query based on these weaknesses, obtaining

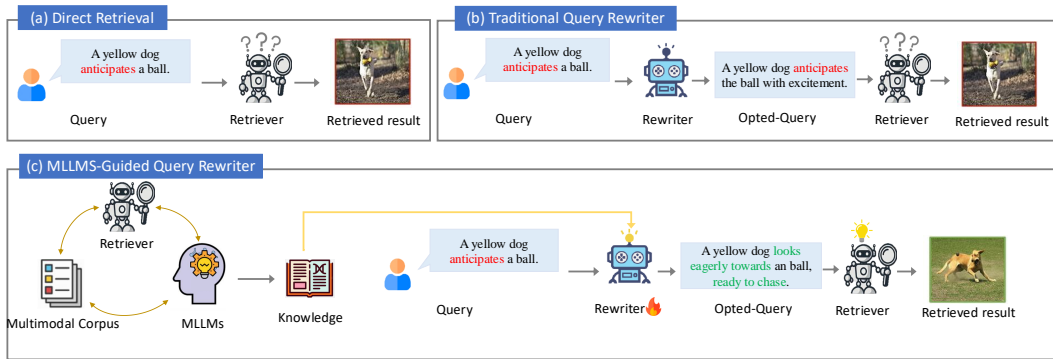


Figure 1: Comparison of different retrieval paradigms. (a) Direct retrieval and (b) traditional rewriting methods yield poor results because the retriever cannot accurately interpret the visual concept “anticipate”. In contrast, our (c) MLLMs-Guided Query Rewriter adapts “anticipate” into a visual description that the retriever understands better, ensuring accurate retrieval.

high-quality queries that match the retriever’s preferences. To distill the preference knowledge into the rewriter, we design a three-step tuning strategy: starting with Supervised Fine-Tuning (SFT) for initial warm-up, followed by Preference Rank Optimization (PRO)(Schulman et al., 2017) to align with the retriever’s fine-grained preferences, and concluding with Proximal Policy Optimization (PPO)(Song et al., 2024) to further enhance the collaboration between the rewriter and the retriever. Through the above training strategies, MGQRe can generate high-quality queries that match the retriever’s preferences. In summary, our contributions are as follows:

- We introduce a novel query optimizer for VLR: MLLMs-Guided Query Rewriter (MGQRe), which refines user-input queries to better align with the preferences of the retriever, thereby enhancing the alignment between the queries and the visual content and improving retrieval performance.
- We develop an automated system for constructing high-quality query datasets for VLR tasks using MLLMs. We deploy MLLMs as agents that analyze the feedback from the retriever to explore its weaknesses and iteratively optimize queries, ensuring that the refined queries align with the retriever’s preferences.
- We develop a three-step learning strategy for the rewriter, consisting of Supervised Fine-Tuning (SFT), Preference Rank Optimization (PRO), and Proximal Policy Optimization (PPO). This strategy enables the rewriter to precisely adjust queries to fit the retriever’s expressive preferences.
- Extensive experiments show that our method significantly outperforms other query optimization methods. Additionally, our method is generalizable and transferable, performing well across various VLR tasks.

2 RELATED WORK

2.1 VISION-LANGUAGE RETRIEVAL

In the task of VLR, the primary objective is to establish alignment between the visual and textual modalities. Previous vision-language models can be categorized into three classes: single-stream, double-stream, and dual-encoder models. Most of the **single-stream** models (Chen et al., 2020; Li et al., 2020; Kim et al., 2021) perform multi-modal interaction via self-attention alignment. These models first concatenate different modalities to produce an integrated sequence, and then perform fine-grained interaction for multi-modal alignment using the transformer’s self-attention. **Double-stream** models (Li et al., 2021; 2022; Yang et al., 2022; Zeng et al., 2022) often apply the intra-modality processing along with a shared fusion encoder. This approach decouples the intra-modal and cross-modal modeling processes. They perform multi-modal interaction via the transformer’s co-attention alignment, where the query vectors are from one modality, and the key and value vec-

108 tors are from the other. Due to the high demand for inference efficiency in visual language retrieval
 109 tasks, some scholars have proposed using the **dual-encoder** architectures for multi-modal alignment
 110 through contrastive learning (Radford et al., 2021; Xie et al., 2022; Ma et al., 2022b). In this
 111 approach, the visual embedding and text embedding are projected into the same semantic space
 112 to calculate similarity scores. Due to their efficient retrieval, dual-stream architectures are gaining
 113 more and more attention in VLR.

114

115 2.2 PROMPT ENGINEERING FOR VISION-LANGUAGE MODEL

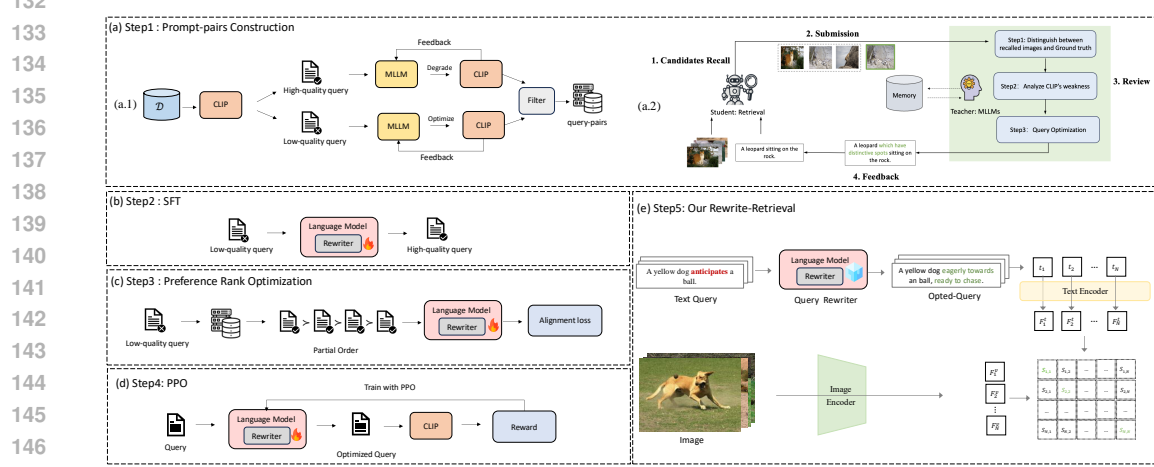
116

117 Prompt engineering has become a vital technique with the rise of large pretrained models, optimizing
 118 queries into formats comprehensible by multimodal models like CLIP. Research mainly focuses
 119 on enhancing model understanding by incorporating additional knowledge, such as entity concepts
 120 from WordNet (Shen et al., 2022; Yao et al., 2022) or domain-specific insights (Ma et al., 2022a).
 121 With the emergence of LLMs, studies increasingly leverage their knowledge bases for query aug-
 122 mentation, including visual descriptions (Menon & Vondrick, 2022; Pratt et al., 2023) to support
 123 text-image alignment. Some research(Xie et al., 2023) also emphasizes retrieval-enhanced tech-
 124 niques that retrieve relevant images for cross-modal understanding. Existing approaches primarily
 125 address image classification and object detection, these coarse-grained methods struggle with com-
 126 plex text queries containing multiple entities and fine-grained interactions. This paper proposes a
 127 fine-grained query optimization scheme for multimodal retrieval, aimed at improving model com-
 128 prehension of complex queries.

129

130 3 METHODOLOGY

131



132

133 Figure 2: The framework of our method. First, we construct the high-/low-quality query pairs by
 134 the interaction of MLLMs and CLIP. Second, we conduct supervised fine-tuning (SFT) for rewriter
 135 on the query pairs. Third, we align fine-grained preferences through preference rank optimiza-
 136 tion. Fourth, we apply Proximal Policy Optimization (PPO) to the rewriter using designed rewards for
 137 further enhancement. Finally, we integrate the rewriter with CLIP to perform VLR.

138

139

140 Given an input query, our prompt optimizer automatically rewrites it to better match the retriever’s
 141 understanding preferences, while preserving the original intent. Fig 2 provides an overview of our
 142 method, with the rewriter built upon a language model. First, we employ MLLMs to capture the
 143 retriever’s preferences and gather high-quality query examples (section 3.1). These examples are
 144 then used to perform Supervised Fine-Tuning (SFT) to prepare the rewriter (section 3.2). To refine
 145 our understanding of the retriever’s fine-grained preferences, we implement Preference Rank Opti-
 146 mization (section 3.3), followed by reinforcement learning to overcome the limitations of synthetic
 147 data (section 3.4). The trained rewriter is then integrated into the multimodal retrieval framework to
 148 perform query optimization (section 3.5).

162
163

3.1 DATASET CONSTRUCTION

164 This section outlines the collection process of data used for training the rewriter. As shown in Fig 2
 165 (a.1), queries that align with the retriever’s preferences are defined as high-quality queries. The
 166 goal of this step is to collect high-quality/low-quality query pairs with similar semantics. The data
 167 originates from Flickr30k and MSCOCO, which contain only unpaired raw queries. Initially, we
 168 categorize the queries into low and high quality based on the evaluation from the retriever.

169 As depicted in Fig 2 (a.2), for low-quality queries, we employ MLLMs as agents to generate high-
 170 quality queries that are easier for the retriever to understand. The specific process includes four steps:
 171 1) Candidate Recall: retrieve candidate images using low-quality queries; 2) Submission: Submit
 172 incorrect candidates and ground truth for comparison; 3) Review: MLLMs optimize and rewrite the
 173 erroneous concepts through chain-of-thought, analyzes the differences between recalled images and
 174 correct images, identifies concepts that retriever failed to understand, and optimizes these deficiencies;
 175 4) Feedback: Retest the rewritten queries to determine if they meet high-quality standards. This
 176 process iterates multiple turns until we get multiple high-quality queries for each low-quality query.
 177 In the above approach, MLLMs identify the retriever’s shortcomings more deeply by analysing hard
 178 negative samples of the retriever, thus more accurately capturing and understanding the retrieval
 179 model’s expression preferences.

180 Similarly, for high-quality queries, we blur concepts using MLLMs and simplify the rewriting of
 181 queries with MLLMs to decrease their similarity to images, thereby generating corresponding low-
 182 quality queries. Finally, we calculate the textual similarity (Reimers, 2019) between low and high-
 183 quality queries and filter out examples with low similarity. Detailed implementation specifics and
 184 prompt templates can be found in the Appendix A.1.

185
186 3.2 SUPERVISED FINE-TUNING

187 With the low-quality/high-quality query pairs established, we can train a query optimizer to develop
 188 basic query optimization capabilities. A parallel query corpus consists of low-quality query x and
 189 high-quality query y , referred to as the D_{SFT} . If a low-quality query x corresponds to multiple
 190 high-quality queries, we take the highest-quality query as y . $\pi(\cdot)$ and θ denote the query rewriter
 191 to be trained during SFT and its parameters, which can be any pretrained language model. We train
 192 the rewriter by minimizing the cross-entropy loss. The training objective for SFT is to optimize the
 193 following loss function:

$$L_{SFT}(\theta) = -\mathbb{E}_{(x,y) \sim D_{SFT}} \sum_t \log \pi(y_t | y_{<t}, x; \theta) \quad (1)$$

194 SFT can be viewed as a warm-up phase, and thus, the effectiveness of the supervised fine-tuning
 195 model is generally moderate. To further enhance model performance, we proceed with preference
 196 optimization.

200
201 3.3 PREFERENCE OPTIMIZATION

202 To enhance the rewriter’s understanding of the model’s fine-grained conceptual preferences, we per-
 203 formed preference optimization. This process requires constructing a dedicated preference dataset
 204 D_{PRO} . As described in Appendix A.1, we generate multiple high-quality queries for each low-
 205 quality query and obtain text-image similarity scores from the retrieval system, which serve as re-
 206 wards for preference learning. These scores allow us to rank the enhanced queries from high to low.
 207 To minimize bias from the reward model and enhance fine-grained preference comparisons from a
 208 global perspective, we introduce Preference Rank Optimization (PRO) based on the Bradley-Terry
 209 model(Song et al., 2024). This method guides the model to learn the ranking of rewrites according
 210 to feedback from the retriever. According to the Bradley-Terry model, the probability of choosing
 211 a policy is proportional to its corresponding reward. Given the partial order relation $y_1 \succ y_2$, the
 212 preference probability can be expressed as:

$$P_{BT} = \frac{\exp(r(y_1, x))}{\exp(r(y_1, x)) + \exp(r(y_2, x))} \quad (2)$$

213 where $r(\cdot)$ is the reward function, which is defined as the normalized log probability of the rewrite
 214 generated in PRO. PRO extends pairwise partial order into general listwise partial order. The PRO

216 loss is expressed by the equation:
 217

$$218 \quad L_{\text{PRO}}(\theta) = -\mathbb{E}_{(\mathbf{x}, \mathbf{y}) \sim D_{\text{PRO}}} \sum_{j=1}^{k-1} \log \frac{\exp\left(\frac{\pi_{\text{PRO}}(y_j | x; \theta)}{T_j^j}\right)}{\sum_{i=j}^k \exp\left(\frac{\pi_{\text{PRO}}(y_i | x; \theta)}{T_j^i}\right)} \quad (3)$$

222 where $T_j^i = \frac{1}{r(y_j) - r(y_i)}$ and $T_j^j = \min_{i>j}(T_j^i)$ are used to measure ranking difference. k denotes the
 223 number of candidate high-quality queries, π_{PRO} and θ refer to the policy model and its parameters.
 224

225 3.4 REINFORCEMENT LEARNING

228 Due to the limited datasets collected and inherent noise, relying solely on constructing query pairs
 229 is insufficient for effectively guiding the rewriter. Consequently, we propose using reinforcement
 230 learning to enable the rewriter to explore freely and better adapt to the retriever. Initially, we define
 231 the rewards for reinforcement learning, focusing on the improvement in cross-modal similarity as a
 232 measure of query quality. The reward is then defined as follows:

$$233 \quad r(x, y) = 20 * (s_{\text{clip}}(y, v_x) - s_{\text{clip}}(x, v_x)) \quad (4)$$

234 where $s_{\text{clip}}(\cdot)$ denotes the similarly score between query and image, v_x represents the ground image
 235 related to query x . After obtaining the predefined reward, we suggest using Proximal Policy Opti-
 236 mization (PPO) during reinforcement learning training to enhance our retriever. The PPO algorithm
 237 directly optimizes the expected reward:

$$239 \quad L_{\text{PPO}}(\theta) = -\mathbb{E}_{\mathbf{x} \sim D_{\text{PPO}}, \mathbf{y} \sim \pi_{\text{PPO}}(\cdot | x)} [r(x, y) - \beta \cdot \log \frac{\pi_{\text{PPO}}(y | x)}{\pi_{\text{PRO}}(y | x)}] \quad (5)$$

241 Following (Ziegler et al., 2019), we adopt an adaptive KL penalty strategy with parameter β , which
 242 is used to prevent the policy from deviating too far from the initial distribution π_{PRO} .
 243

244 3.5 INTEGRATION OF THE REWRITER FOR VLR

246 In our work, we select the simple yet effective dual-encoder model CLIP as the foundational model
 247 (a detailed introduction and training for CLIP can be found in Appendix A.2). We incorporate the
 248 trained rewriter into the CLIP framework, as illustrated in Fig 2 (e). During CLIP fine-tuning, we
 249 freeze the rewriter and randomly perform query rewriting with probability p . For inference, given
 250 an input text query, we utilize the rewriter to generate the opted-query. This opted-query is modeled
 251 through the text encoder to obtain text feature, which is then computed with the features of candidate
 252 images for similarity score. Finally, images are recalled in descending order of similarity.

253 4 EXPERIMENTS

254 4.1 EXPERIMENT SETTING

255 4.1.1 DATASETS

256 We primarily evaluate on two benchmark datasets: Flickr30k and MSCOCO, to validate its effec-
 257 tiveness. (1) **Flickr30k** (Plummer et al., 2015) contains 31,000 images, each with 5 captions, and is
 258 divided into 29K/1K/1K images for training, validation, and testing, respectively (Li et al., 2021). (2)
 259 **MSCOCO** (Lin et al., 2014) consists of 123,287 images, also with 5 captions each, and is split into
 260 114K/5K/5K for training, validation, and testing. To further assess the transferability of our method,
 261 we evaluate its performance on other visual-text retrieval datasets, including (3) **MSR-VTT** (Xu
 262 et al., 2016), which includes 10,000 videos with a total of 200,000 text descriptions. We utilize 9K
 263 videos for training and evaluation on a 1K test set. Additionally, (4) **SBU30k** (Ordonez et al., 2011)
 264 contains 36,000 image-text pairs randomly sampled from SBU Captions, divided into 30K/3K/3K
 265 for training, validation, and testing. Furthermore, we randomly sample from CC12M (Changpinyo
 266 et al., 2021) and YFCC15M (Thomee et al., 2016) to obtain (5) **CC30K** and (6) **YFCC30K**. Details
 267 on the query pair dataset constructed for the rewriter can be seen in Appendix A.1.
 268

270 4.1.2 BASELINES
271

272 We will validate our method on advanced dual-encoder retrieval models, specifically: (1)
 273 **CLIP**(Radford et al., 2021), a powerful dual-encoder model pre-trained through contrastive learning;
 274 (2) **CoCa**(Yu et al., 2022), a framework that integrates various pre-training paradigms, utilizing
 275 its image encoder and unimodal text decoder for retrieval; and (3) **EVA-02-CLIP** (Sun et al., 2023),
 276 which employs novel representation learning techniques to enhance CLIP’s performance.

277 Our approach will be compared with current query optimization methods, including: (1) **Det-CLIP**
 278 (Yao et al., 2022): An entity knowledge enhancement method that integrates WordNet conceptual
 279 knowledge into query entities. (2) **CLIP-GPT** (Maniparambil et al., 2023) An entity description
 280 enhancement scheme that incorporates visual descriptions generated by LLMs into query entities.
 281 (3) **RACLIP** (Xie et al., 2023): A retrieval augmentation approach that uses relevant images to en-
 282 rich the query with cross-modal semantics. (4) **LLMsRewrite**: A description rewriting scheme that
 283 utilizes LLMs for query optimization. We have designed templates to guide LLMs, which include
 284 task descriptions and crafted examples.

285 To evaluate the effectiveness of our dataset generation strategy, we compared three dataset construction
 286 scenarios: (1) **Direct Generation Strategy**: Queries are generated directly based on image
 287 content using MLLMs. (2) **Feedback Enhancement Strategy**: MLLMs generate queries based
 288 on the image, then refine these queries using the in-retriever similarity score between the generated
 289 query and the image as a metric for feedback and subsequent optimization. (3) **Challenge Response**
 290 **Strategy**: Our implementation involves using challenging negative and positive samples from the
 291 retriever to identify its weaknesses, allowing for continuous query adjustment and optimization.

292 In addition, we explore various open-source LLMs for rewriters, including Qwen-7B (Bai et al.,
 293 2023) (“Qwen-7B-chat”), Baichuan2-7B (Yang et al., 2023) (“Baichuan2-7B-chat”), Llama (Tou-
 294 vron et al., 2023) (“Llama2-7B-chat”), and Vicuna (Chiang et al., 2023) (“vicuna-7B-v1.3”).

295 4.1.3 IMPLEMENTATION DETAILS
296

297 We fine-tune a pre-trained retrieval (e.g., CLIP) directly without the pretraining, making the process
 298 lightweight. The settings for fine-tuning the retrieval are as follows: we use the Adam optimizer
 299 with a weight decay of 1e-3 and a batch size of 256. The total number of fine-tuning epochs is set to
 300 20. The initial learning rate is 1e-6, with a cosine learning rate scheduler, and a warm-up strategy is
 301 applied for the first 2k steps. The probability of random rewriting during retrieval fine-tuning p is set
 302 to 0.6. In our experiments, the visual encoder includes two variants: Vision Transformer (ViT-B/32,
 303 ViT-B/16, and ViT-L/14) and ResNet (RN50 and RN101). For the text encoder, we use the vanilla
 304 Transformer from CLIP (Vaswani et al., 2017). Input images are resized to 224×224 , and input
 305 sequences are truncated or padded to 77 tokens.

306 For the prompt-pairs construction, we use GPT-4V as the MLLM. The details for constructing low-
 307 quality/high-quality query pairs can be found in Appendix A.1. Unless otherwise specified, we use
 308 Llama2-7b as the query rewriter. For the SFT phase, we set the learning rate to 1e-5, the batch size
 309 to 32, and run for 10 epochs. In the DPO phase, the learning rate is set to 5e-7, with a batch size
 310 of 16, across 5 epochs, and a rank length of 5. For the PPO phase, CLIP with ViT-B/32 is used
 311 for reward calculation. The learning rate is set to 5e-6, with a batch size of 32, and 1 epoch of
 312 fine-tuning. The KL coefficient β is set to 0.1. Following previous work (Radford et al., 2021), we
 313 use recall R@ h ($h = 1, 5, 10$) as the evaluation metric.

314 4.2 MAIN RESULT
315

316 We conduct evaluations of our method on two benchmark datasets, Flickr30K and MSCOCO, uti-
 317 lizing advanced VLR dual-encoder frameworks. As shown in Table 1, we compare various query
 318 optimization methods, analyzing the results to draw several conclusions:

319 **Entity Enhancement Surpass Image Retrieval Enhancements**: Our experiments demonstrate
 320 that various query optimization methods enhance vision-language retrieval performance. Notably,
 321 methods incorporating entity visual descriptions (CLIP-GPT) and entity knowledge (DetCLIP) sig-
 322 nificantly outperform enhancements based on related images (RACLIP). We speculate that because
 323 the description of entities and knowledge are more granular than the global information provided by

Table 1: Fine-tuning results for image-text retrieval on the Flickr30K (1K) test set and MSCOCO (5K) test set. Notations: V-Encoder: vision encoder; # PT Data: the pre-training datasets.

| Methods | V-Encoder | # PT Data | Flickr30K(1K) | | | | | | MSCOCO(5K) | | | | | |
|-----------------|-----------|-----------|---------------|-------------|-------------|---------------|-------------|-------------|---------------|-------------|-------------|---------------|-------------|-------------|
| | | | I2T Retrieval | | | T2I Retrieval | | | I2T Retrieval | | | T2I Retrieval | | |
| | | | R@1 | R@5 | R@10 |
| CLIP | ViT-B/32 | NA | 64.8 | 85.7 | 92.5 | 49.2 | 79.3 | 86.8 | 43.7 | 73.5 | 82.6 | 32.7 | 63.3 | 75.0 |
| DetCLIP | ViT-B/32 | NA | 65.2 | 86.3 | 93.5 | 50.7 | 79.2 | 86.8 | 45.2 | 73.7 | 83.4 | 33.4 | 63.5 | 75.0 |
| CLIP-GPT | ViT-B/32 | NA | 66.5 | 88.1 | 93.6 | 51.2 | 80.1 | 87.8 | 46.1 | 74.0 | 83.7 | 34.1 | 63.7 | 75.3 |
| RACLIP | ViT-B/32 | NA | 65.1 | 86.2 | 93.0 | 50.2 | 79.4 | 87.1 | 45.1 | 73.6 | 82.7 | 33.1 | 63.4 | 74.9 |
| LLMsRewrite | ViT-B/32 | NA | 66.5 | 87.6 | 93.3 | 50.8 | 79.8 | 87.3 | 45.7 | 73.9 | 83.5 | 33.5 | 63.5 | 75.1 |
| MGQRe | ViT-B/32 | NA | 67.1 | 88.7 | 94.2 | 52.2 | 80.6 | 87.7 | 46.7 | 74.6 | 84.3 | 35.2 | 64.4 | 75.8 |
| CLIP | ViT-B/32 | Laion400M | 89.1 | 97.8 | 98.9 | 74.1 | 92.6 | 95.9 | 65.3 | 85.9 | 91.9 | 48.1 | 75.0 | 83.7 |
| DetCLIP | ViT-B/32 | Laion400M | 89.2 | 97.8 | 99.1 | 74.6 | 92.8 | 96.0 | 65.5 | 85.9 | 92.1 | 48.3 | 75.1 | 83.7 |
| CLIP-GPT | ViT-B/32 | Laion400M | 89.7 | 98.7 | 99.2 | 75.2 | 93.1 | 96.1 | 66.2 | 86.2 | 92.3 | 48.8 | 75.3 | 84.3 |
| RACLIP | ViT-B/32 | Laion400M | 89.2 | 98.0 | 98.9 | 74.4 | 92.8 | 96.0 | 65.3 | 86.1 | 92.1 | 48.5 | 75.2 | 83.8 |
| LLMsRewrite | ViT-B/32 | Laion400M | 89.3 | 98.1 | 99.0 | 74.5 | 92.9 | 96.0 | 65.3 | 86.0 | 91.9 | 48.3 | 75.2 | 84.0 |
| MGQRe | ViT-B/32 | Laion400M | 90.8 | 99.2 | 99.6 | 75.7 | 93.6 | 96.5 | 66.8 | 86.9 | 92.7 | 49.5 | 76.0 | 84.6 |
| CoCa | ViT-B/32 | Laion-2B | 85.5 | 96.5 | 98.7 | 72.0 | 91.2 | 95.4 | 63.9 | 85.6 | 91.0 | 45.6 | 72.1 | 82.2 |
| DetCoCa | ViT-B/32 | Laion-2B | 85.6 | 96.5 | 98.7 | 72.2 | 91.2 | 95.4 | 63.8 | 85.5 | 91.0 | 45.8 | 72.1 | 82.1 |
| CoCa-GPT | ViT-B/32 | Laion-2B | 86.2 | 97.0 | 98.8 | 72.2 | 91.6 | 95.3 | 64.3 | 85.7 | 91.0 | 46.0 | 72.2 | 82.3 |
| RACoCa | ViT-B/32 | Laion-2B | 85.8 | 96.6 | 98.8 | 72.1 | 91.2 | 95.3 | 64.1 | 85.6 | 91.1 | 45.7 | 72.1 | 82.0 |
| LLMsRewrite | ViT-B/32 | Laion-2B | 86.1 | 96.7 | 98.8 | 72.1 | 91.3 | 95.5 | 64.2 | 85.6 | 91.1 | 45.8 | 72.1 | 82.2 |
| MGQRe | ViT-B/32 | Laion-2B | 86.8 | 97.3 | 98.9 | 72.7 | 91.6 | 95.8 | 65.0 | 85.9 | 91.5 | 46.6 | 72.7 | 82.5 |
| EVA-02-CLIP | ViT-B/16 | Merged-2B | 90.8 | 98.7 | 99.2 | 78.9 | 94.7 | 97.0 | 69.1 | 89.2 | 94.0 | 52.6 | 78.5 | 86.8 |
| DetEVA-02-CLIP | ViT-B/16 | Merged-2B | 90.9 | 98.6 | 99.1 | 79.1 | 94.6 | 97.0 | 69.3 | 89.2 | 94.0 | 52.7 | 78.5 | 86.7 |
| EVA-02-CLIP-GPT | ViT-B/16 | Merged-2B | 91.1 | 98.7 | 99.2 | 79.3 | 94.7 | 97.1 | 69.4 | 89.3 | 94.3 | 52.6 | 78.6 | 86.8 |
| RAEVA-02-CLIP | ViT-B/16 | Merged-2B | 90.7 | 98.6 | 99.1 | 79.0 | 94.6 | 97.0 | 69.1 | 89.0 | 94.0 | 52.6 | 78.5 | 86.6 |
| LLMsRewrite | ViT-B/16 | Merged-2B | 91.0 | 98.6 | 99.2 | 79.2 | 94.7 | 97.0 | 69.2 | 89.2 | 94.1 | 52.8 | 78.6 | 86.8 |
| MGQRe | ViT-B/16 | Merged-2B | 91.5 | 98.7 | 99.5 | 79.7 | 95.0 | 97.3 | 69.9 | 89.8 | 94.4 | 53.6 | 79.1 | 87.2 |

images, they better capture the fine-grained cues required for text-image alignment. In VLR, visual description of entities proves more advantageous than conceptual knowledge, because it provides more detailed perceptual information that helps the model capture specific visual details.

MGQRe Outperforms All Existing Approaches: As shown in Table 1, our method (MGQRe) improves the retrieve’s performance best. Compared to entity enhancement methods that provide only entity knowledge and retrieval enhancement methods that provide global coarse-grained perception, our approach can optimize fine-grained concepts within queries, covering not only entities but also interactive and descriptive concepts. Therefore, our method displays superior performance in multimodal retrieval tasks.

Unoptimized rewriters (LLMsRewrite) show underperformance in VLR. The main reason is that these rewriters do not adjust based on retriever’s feedback, thus generating queries that may not align with the retriever’s understand preferences, and may even distort the original queries’ intent. MGQRe, learning from retriever’s preferences, identifies which expressions are more effective for retrievers and performs targeted optimizations, thus enhancing queries’ quality.

Significant Improvements Across Different Retrievers: Further experiments on CLIP-like models, detailed in Table 1, demonstrated that models like CoCa and EVA-02-CLIP achieved significant performance improvements on most metrics after adopting our method. This underscores our approach’s generalizability and effectiveness. Furthermore, in Appendix A.3, we show that our method is applicable to retrievers with various vision encoders.

4.3 ABLATION STUDY

Using CLIP with ViT-B/32, pre-trained on Laion400M, as our baseline, we conducted comprehensive ablation studies on MGQRe to evaluate the impact of data collection, training strategies, and large language models on performance.

Table 2: Ablation studies on dataset collection strategies. The Fine-tuning dataset is Flickr30k.

| Methods | I2T Retrieval R@1 R@5 | T2I Retrieval R@1 R@5 |
|----------------------|-----------------------------|-----------------------------|
| Baseline | 89.1 97.8 | 74.1 92.6 |
| Direct Generation | 89.2 98.1 | 74.5 92.8 |
| Feedback Enhancement | 90.5 98.8 | 75.1 93.4 |
| Challenge Response | 90.8 99.2 | 75.7 93.6 |

| Methods | I2T Retrieval R@1 R@5 | T2I Retrieval R@1 R@5 |
|-----------------|-----------------------------|-----------------------------|
| Freeze | 89.3 98.1 | 74.5 92.9 |
| SFT | 89.6 98.4 | 75.0 93.3 |
| SFT + PRO | 90.4 98.9 | 75.3 93.6 |
| SFT + PRO + PPO | 90.8 99.2 | 75.7 93.6 |

378 4.3.1 DATA COLLECTION STRATEGIES
 379

380 In this section, we evaluate different data generation strategies. As shown in Table 2, Direct Generation
 381 ignores the preferences of the retrieval model, resulting in limited performance improvements
 382 due to the lack of task-specific tuning. Feedback Enhancement considers the retrieval model’s pre-
 383 ferences during query rewriting but fails to explore the model’s weaknesses, limiting its effective-
 384 ness in more challenging scenarios. Challenge Response leverages MLLMs to analyze the model’s
 385 weaknesses by focusing on difficult negative and positive samples, enabling targeted optimization
 386 to address these shortcomings and further enhance overall performance.
 387

388 4.3.2 TRAINING STRATEGIES
 389

390 We conducted ablation studies on different training strategies to assess their impact on the perfor-
 391 mance of our rewriter. The experimental results are shown in Table 3.
 392

393 Initially, using only Supervised Fine-Tuning (SFT), the model demonstrated basic rewriting capa-
 394 bilities and adapted to preliminary query optimization. However, this method had its limitations
 395 as it relied heavily on existing data, preventing the model from fully understanding the retriever’s
 396 fine-grained preferences and thus limiting performance improvements. By incorporating Prefer-
 397 ence Rank Optimization (PRO), the model gained a deeper understanding of the retriever’s detailed
 398 preferences, enabling the generation of higher-quality queries and significantly enhanced retrieval
 399 performance. Finally, the introduction of reinforcement learning overcame the limitations of data,
 400 allowing the model to dynamically explore and adapt to the retriever’s preferences, further improving
 401 performance. This progression illustrates the effectiveness of layering advanced learning strategies
 402 to significantly boost the capabilities of the query rewriter.

402 Table 4: Ablation studies on language mod-
 403 els. The Fine-tuning dataset is Flickr30k.
 404

| Methods | LLMs | I2T Retrieval | | | T2I Retrieval | | |
|---------|--------------|---------------|-------------|-------------|---------------|-------------|-------------|
| | | R@1 | R@5 | R@10 | R@1 | R@5 | R@10 |
| CLIP | NA | 89.1 | 97.8 | 98.9 | 74.1 | 92.6 | 95.9 |
| MGQRe | Vicuna-7B | 90.5 | 99.1 | 99.3 | 75.2 | 93.3 | 96.4 |
| | Baichuan2-7B | 90.5 | 99.0 | 99.5 | 75.5 | 93.3 | 96.5 |
| | Qwen-7B | 90.6 | 98.9 | 99.4 | 75.6 | 93.4 | 96.4 |
| | LLama2-7B | 90.8 | 99.2 | 99.6 | 75.7 | 93.6 | 96.5 |
| | LLama2-13B | 90.9 | 99.2 | 99.6 | 75.8 | 93.7 | 96.5 |

Table 5: Performance on various VLR datasets.

| Data | Methods | I2T Retrieval | | | T2I/T2V Retrieval | | |
|---------|---------|---------------|-------------|-------------|-------------------|-------------|-------------|
| | | R@1 | R@5 | R@10 | R@1 | R@5 | R@10 |
| MSR-VTT | CLIP | - | - | - | 34.6 | 63.1 | 73.7 |
| | MGQRe | - | - | - | 35.8 | 63.8 | 74.7 |
| CC30k | CLIP | 59.0 | 81.2 | 88.3 | 58.5 | 80.5 | 87.1 |
| | MGQRe | 61.2 | 81.8 | 88.5 | 59.8 | 81.5 | 87.6 |
| SBU30k | CLIP | 43.8 | 66.3 | 74.3 | 43.4 | 65.7 | 74.4 |
| | MGQRe | 45.2 | 67.7 | 75.3 | 44.7 | 67.3 | 74.6 |
| YFCC30k | CLIP | 37.4 | 56.3 | 64.3 | 35.8 | 56.6 | 64.6 |
| | MGQRe | 39.1 | 56.7 | 64.7 | 36.6 | 57.2 | 64.4 |

411 4.3.3 LARGE LANGUAGE MODELS
 412

413 We conduct ablation studies using various large language models as rewriters to assess the capa-
 414 bilities and limitations of query editing techniques. As shown in Table 4, the performance across
 415 all tested LLMs is relatively consistent, with LLama2 showing significantly better results. Import-
 416 antly, the performance of LLama2-7B is comparable to that of LLama2-13B, suggesting that under
 417 our training strategy, smaller language models are sufficiently effective for query optimization tasks
 418 without significantly impacting efficiency. This finding highlights the potential for optimising re-
 419 trieval efficiency without compromising the quality of queries.
 420

421 4.4 TRANSFERABLE OF REWRITER
 422

423 We further explore the transferability of our rewriter across various visual language retrieval datasets.
 424 As shown in Table 5, we perform experimental validations on the video-text retrieval dataset MSR-
 425 VTT as well as other image-text retrieval datasets. Despite the rewriter being trained on the
 426 Flickr30K and MSCOCO datasets, it still enhances the performance of the retrievers on these differ-
 427 ent datasets.
 428

429 This result shows that the model preferences and optimisation capabilities learned by the rewriter
 430 from a specific dataset are transferable. These capabilities can be effectively transferred to other
 431 visual language retrieval tasks, indicating that the rewriter has broad applicability in improving the
 432 retrieval performance of diverse visual language datasets.

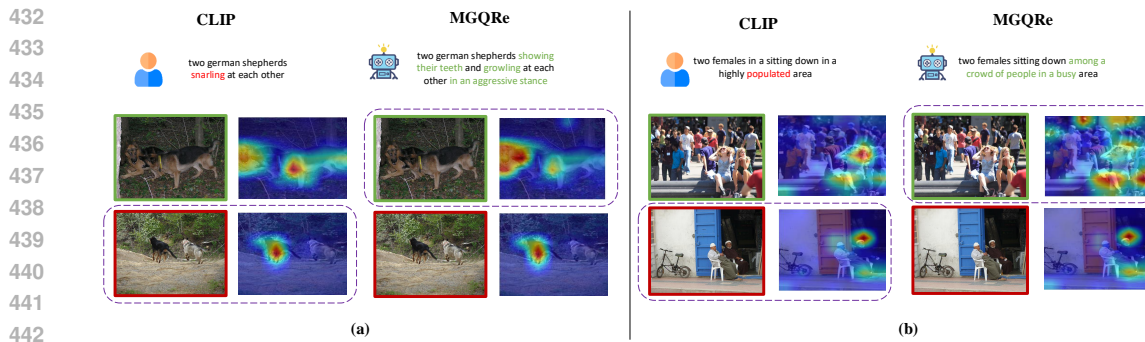


Figure 3: Visualization example of text-to-image retrieval, showcasing heatmaps corresponding to different text queries. The image inside the dashed box is the retrieved result of the query. MGQRe optimizes user-input queries into queries that are more comprehensible to the retriever, facilitating better alignment between the queries and the visual content of images.

4.5 VISUALIZATION ANALYSIS

To gain a deeper understanding of how MGQRe improves the matching of queries to images, we have visually demonstrated that MGQRe helps the retriever to focus on image regions relevant to the query semantics. We utilize the Integrated Gradients algorithm (Qi et al., 2019), which calculates and evaluates the impact of each feature on the final prediction.

As shown in Fig 3 (a), the heatmap clearly indicates that CLIP struggles with the visual concept of “snarling”, as it fails to match “snarling” with the corresponding visual content in the image, leading to inaccurate retrieval results. MGQRe optimizes the query by rewriting “snarling” into a more retriever-friendly visual description, such as “showing their teeth”. This helps the retriever better understand the concept and focus its attention on the relevant visual content, resulting in accurate retrieval. Similarly, Fig 3 (b) demonstrates that CLIP also has difficulty aligning the term “populated” with its corresponding visual content. MGQRe optimizes the query into a description that fits CLIP’s visual preferences, aiding the retriever in more accurately aligning the query with the image content. This visualization underscores MGQRe’s effectiveness in improving retrieval accuracy by refining queries to match the retriever’s comprehension preferences.

4.6 LIMITATIONS

While MGQRe effectively rewrites queries to align better with the preferences of the retriever, it can occasionally introduce additional information that may act as noise in multimodal matching, potentially affecting the performance of cross-modal alignment. Addressing this issue is a key direction for future optimization. Additionally, MGQRe faces challenges in retrieval efficiency. We believe that with the rapid advancement in large language models, the emergence of more lightweight, high-performance language models (Hu et al., 2024) will gradually mitigate this issue.

5 CONCLUSION

In this paper, we introduce a query optimizer named MGQRe for visual-text retrieval, designed to rewrite query concepts that are difficult for retrievers to understand into expressions that align with their comprehension preferences. Specifically, we utilize multimodal large language models to capture the preferences of retrievers, analyze their performance weaknesses, and iteratively optimize to generate high-quality queries that meet these preferences. We then implement a three-phase optimization strategy that effectively distills the retriever’s preferences into the rewriter, ensuring that user-input queries are optimized into forms more easily understood by the retriever. Extensive experimental results demonstrate that our method outperforms other query optimization strategies, showcasing strong generalizability and transferability. These contributions provide valuable insights for future research in visual-text retrieval. Future research directions could further explore how to integrate user preferences and domain-specific knowledge into the rewriter to enrich the application scenarios of query optimization in multimodal retrieval.

486 REFERENCES
487

488 Jinze Bai, Shuai Bai, Yunfei Chu, Zeyu Cui, Kai Dang, Xiaodong Deng, Yang Fan, Wenbin Ge,
489 Yu Han, Fei Huang, et al. Qwen technical report. *arXiv preprint arXiv:2309.16609*, 2023.

490 Soravit Changpinyo, Piyush Sharma, Nan Ding, and Radu Soricut. Conceptual 12m: Pushing
491 web-scale image-text pre-training to recognize long-tail visual concepts. In *Proceedings of the*
492 *IEEE/CVF Conference on Computer Vision and Pattern Recognition*, pp. 3558–3568, 2021.
493

494 Yen-Chun Chen, Linjie Li, Licheng Yu, Ahmed El Kholy, Faisal Ahmed, Zhe Gan, Yu Cheng, and
495 Jingjing Liu. Uniter: Universal image-text representation learning. In *Computer Vision–ECCV*
496 *2020: 16th European Conference, Glasgow, UK, August 23–28, 2020, Proceedings, Part XXX*,
497 pp. 104–120. Springer, 2020.

498 Wei-Lin Chiang, Zhuohan Li, Zi Lin, Ying Sheng, Zhanghao Wu, Hao Zhang, Lianmin Zheng,
499 Siyuan Zhuang, Yonghao Zhuang, Joseph E Gonzalez, et al. Vicuna: An open-source chatbot
500 impressing gpt-4 with 90%* chatgpt quality. See <https://vicuna.lmsys.org> (accessed 14 April
501 2023), 2023.

502 Kai Han, Yunhe Wang, Hanting Chen, Xinghao Chen, Jianyuan Guo, Zhenhua Liu, Yehui Tang,
503 An Xiao, Chunjing Xu, Yixing Xu, et al. A survey on vision transformer. *IEEE transactions on*
504 *pattern analysis and machine intelligence*, 45(1):87–110, 2022.

505 Kaiming He, Xiangyu Zhang, Shaoqing Ren, and Jian Sun. Deep residual learning for image recog-
506 nition. In *Proceedings of the IEEE conference on computer vision and pattern recognition*, pp.
507 770–778, 2016.

508 Shengding Hu, Yuge Tu, Xu Han, Chaoqun He, Ganqu Cui, Xiang Long, Zhi Zheng, Yewei Fang,
509 Yuxiang Huang, Weilin Zhao, et al. Minicpm: Unveiling the potential of small language models
510 with scalable training strategies. *arXiv preprint arXiv:2404.06395*, 2024.

511 Yizhang Jin, Jian Li, Yexin Liu, Tianjun Gu, Kai Wu, Zhengkai Jiang, Muyang He, Bo Zhao, Xin
512 Tan, Zhenye Gan, et al. Efficient multimodal large language models: A survey. *arXiv preprint*
513 *arXiv:2405.10739*, 2024.

514 Wonjae Kim, Bokyung Son, and Ildoo Kim. Vilt: Vision-and-language transformer without convo-
515 lution or region supervision. In *International Conference on Machine Learning*, pp. 5583–5594.
516 PMLR, 2021.

517 Junnan Li, Ramprasaath Selvaraju, Akhilesh Gotmare, Shafiq Joty, Caiming Xiong, and Steven
518 Chu Hong Hoi. Align before fuse: Vision and language representation learning with momentum
519 distillation. *Advances in neural information processing systems*, 34:9694–9705, 2021.

520 Junnan Li, Dongxu Li, Caiming Xiong, and Steven Hoi. Blip: Bootstrapping language-image pre-
521 training for unified vision-language understanding and generation. In *International Conference*
522 *on Machine Learning*, pp. 12888–12900. PMLR, 2022.

523 Xiujun Li, Xi Yin, Chunyuan Li, Pengchuan Zhang, Xiaowei Hu, Lei Zhang, Lijuan Wang, Houdong
524 Hu, Li Dong, Furu Wei, et al. Oscar: Object-semantics aligned pre-training for vision-language
525 tasks. In *Computer Vision–ECCV 2020: 16th European Conference, Glasgow, UK, August 23–28,*
526 *2020, Proceedings, Part XXX 16*, pp. 121–137. Springer, 2020.

527 Tsung-Yi Lin, Michael Maire, Serge Belongie, James Hays, Pietro Perona, Deva Ramanan, Piotr
528 Dollár, and C Lawrence Zitnick. Microsoft coco: Common objects in context. In *Computer*
529 *Vision–ECCV 2014: 13th European Conference, Zurich, Switzerland, September 6–12, 2014,*
530 *Proceedings, Part V 13*, pp. 740–755. Springer, 2014.

531 Haoyu Ma, Handong Zhao, Zhe Lin, Ajinkya Kale, Zhangyang Wang, Tong Yu, Jiuxiang Gu, Sunav
532 Choudhary, and Xiaohui Xie. Ei-clip: Entity-aware interventional contrastive learning for e-
533 commerce cross-modal retrieval. In *Proceedings of the IEEE/CVF Conference on Computer Vi-*
534 *sion and Pattern Recognition*, pp. 18051–18061, 2022a.

- 540 Yiwei Ma, Guohai Xu, Xiaoshuai Sun, Ming Yan, Ji Zhang, and Rongrong Ji. X-clip: End-to-
 541 end multi-grained contrastive learning for video-text retrieval. In *Proceedings of the 30th ACM*
 542 *International Conference on Multimedia*, pp. 638–647, 2022b.
- 543
 544 Mayug Maniparambil, Chris Vorster, Derek Molloy, Noel Murphy, Kevin McGuinness, and Noel E
 545 O’Connor. Enhancing clip with gpt-4: Harnessing visual descriptions as prompts. In *Proceedings*
 546 *of the IEEE/CVF International Conference on Computer Vision*, pp. 262–271, 2023.
- 547 Sachit Menon and Carl Vondrick. Visual classification via description from large language models.
 548 *arXiv preprint arXiv:2210.07183*, 2022.
- 549
 550 Vicente Ordonez, Girish Kulkarni, and Tamara Berg. Im2text: Describing images using 1 million
 551 captioned photographs. *Advances in neural information processing systems*, 24, 2011.
- 552 Bryan A Plummer, Liwei Wang, Chris M Cervantes, Juan C Caicedo, Julia Hockenmaier, and Svet-
 553 lana Lazebnik. Flickr30k entities: Collecting region-to-phrase correspondences for richer image-
 554 to-sentence models. In *Proceedings of the IEEE international conference on computer vision*, pp.
 555 2641–2649, 2015.
- 556 Sarah Pratt, Ian Covert, Rosanne Liu, and Ali Farhadi. What does a platypus look like? gener-
 557 ating customized prompts for zero-shot image classification. In *Proceedings of the IEEE/CVF*
 558 *International Conference on Computer Vision*, pp. 15691–15701, 2023.
- 559
 560 Zhongang Qi, Saeed Khorram, and Fuxin Li. Visualizing deep networks by optimizing with inte-
 561 grated gradients. In *CVPR Workshops*, volume 2, pp. 1–4, 2019.
- 562 Alec Radford, Jong Wook Kim, Chris Hallacy, Aditya Ramesh, Gabriel Goh, Sandhini Agarwal,
 563 Girish Sastry, Amanda Askell, Pamela Mishkin, Jack Clark, et al. Learning transferable visual
 564 models from natural language supervision. In *International conference on machine learning*, pp.
 565 8748–8763. PMLR, 2021.
- 566
 567 N Reimers. Sentence-bert: Sentence embeddings using siamese bert-networks. *arXiv preprint*
 568 *arXiv:1908.10084*, 2019.
- 569
 570 John Schulman, Filip Wolski, Prafulla Dhariwal, Alec Radford, and Oleg Klimov. Proximal policy
 571 optimization algorithms. *arXiv preprint arXiv:1707.06347*, 2017.
- 572
 573 Sheng Shen, Chunyuan Li, Xiaowei Hu, Yujia Xie, Jianwei Yang, Pengchuan Zhang, Zhe Gan,
 574 Lijuan Wang, Lu Yuan, Ce Liu, et al. K-lite: Learning transferable visual models with external
 575 knowledge. *Advances in Neural Information Processing Systems*, 35:15558–15573, 2022.
- 576
 577 Feifan Song, Bowen Yu, Minghao Li, Haiyang Yu, Fei Huang, Yongbin Li, and Houfeng Wang.
 578 Preference ranking optimization for human alignment. In *Proceedings of the AAAI Conference*
 579 *on Artificial Intelligence*, volume 38, pp. 18990–18998, 2024.
- 580
 581 Quan Sun, Yuxin Fang, Ledell Wu, Xinlong Wang, and Yue Cao. Eva-clip: Improved training
 582 techniques for clip at scale. *arXiv preprint arXiv:2303.15389*, 2023.
- 583
 584 Bart Thomee, David A Shamma, Gerald Friedland, Benjamin Elizalde, Karl Ni, Douglas Poland,
 585 Damian Borth, and Li-Jia Li. Yfcc100m: The new data in multimedia research. *Communications*
 586 *of the ACM*, 59(2):64–73, 2016.
- 587
 588 Hugo Touvron, Louis Martin, Kevin Stone, Peter Albert, Amjad Almahairi, Yasmine Babaei, Niko-
 589 lay Bashlykov, Soumya Batra, Prajjwal Bhargava, Shruti Bhosale, et al. Llama 2: Open founda-
 590 tion and fine-tuned chat models. *arXiv preprint arXiv:2307.09288*, 2023.
- 591
 592 Ashish Vaswani, Noam Shazeer, Niki Parmar, Jakob Uszkoreit, Llion Jones, Aidan N Gomez,
 593 Łukasz Kaiser, and Illia Polosukhin. Attention is all you need. *Advances in neural informa-*
594 tion processing systems, 30, 2017.
- 595
 596 Yiqi Wang, Wentao Chen, Xiaotian Han, Xudong Lin, Haiteng Zhao, Yongfei Liu, Bohan Zhai,
 597 Jianbo Yuan, Quanzeng You, and Hongxia Yang. Exploring the reasoning abilities of multimodal
 598 large language models (mllms): A comprehensive survey on emerging trends in multimodal rea-
 599 soning. *arXiv preprint arXiv:2401.06805*, 2024.

- 594 Chen-Wei Xie, Jianmin Wu, Yun Zheng, Pan Pan, and Xian-Sheng Hua. Token embeddings align-
 595 ment for cross-modal retrieval. In *Proceedings of the 30th ACM International Conference on*
 596 *Multimedia*, pp. 4555–4563, 2022.
- 597 Chen-Wei Xie, Siyang Sun, Xiong Xiong, Yun Zheng, Deli Zhao, and Jingren Zhou. Ra-clip:
 598 Retrieval augmented contrastive language-image pre-training. In *Proceedings of the IEEE/CVF*
 599 *Conference on Computer Vision and Pattern Recognition*, pp. 19265–19274, 2023.
- 600 Jun Xu, Tao Mei, Ting Yao, and Yong Rui. Msr-vtt: A large video description dataset for bridging
 601 video and language. In *Proceedings of the IEEE conference on computer vision and pattern*
 602 *recognition*, pp. 5288–5296, 2016.
- 603 Aiyuan Yang, Bin Xiao, Bingning Wang, Borong Zhang, Ce Bian, Chao Yin, Chenxu Lv, Da Pan,
 604 Dian Wang, Dong Yan, et al. Baichuan 2: Open large-scale language models. *arXiv preprint*
 605 *arXiv:2309.10305*, 2023.
- 606 Jinyu Yang, Jiali Duan, Son Tran, Yi Xu, Sampath Chanda, Liqun Chen, Belinda Zeng, Trishul
 607 Chilimbi, and Junzhou Huang. Vision-language pre-training with triple contrastive learning.
 608 In *Proceedings of the IEEE/CVF Conference on Computer Vision and Pattern Recognition*, pp.
 609 15671–15680, 2022.
- 610 Lewei Yao, Jianhua Han, Youpeng Wen, Xiaodan Liang, Dan Xu, Wei Zhang, Zhenguo Li, Chunjing
 611 Xu, and Hang Xu. Detclip: Dictionary-enriched visual-concept paralleled pre-training for open-
 612 world detection. *arXiv preprint arXiv:2209.09407*, 2022.
- 613 Jiahui Yu, Zirui Wang, Vijay Vasudevan, Legg Yeung, Mojtaba Seyedhosseini, and Yonghui
 614 Wu. Coca: Contrastive captioners are image-text foundation models. *arXiv preprint*
 615 *arXiv:2205.01917*, 2022.
- 616 Yan Zeng, Xinsong Zhang, and Hang Li. Multi-grained vision language pre-training: Aligning
 617 texts with visual concepts. In *International Conference on Machine Learning*, pp. 25994–26009.
 618 PMLR, 2022.
- 619 Daniel M Ziegler, Nisan Stiennon, Jeffrey Wu, Tom B Brown, Alec Radford, Dario Amodei, Paul
 620 Christiano, and Geoffrey Irving. Fine-tuning language models from human preferences. *arXiv*
 621 *preprint arXiv:1909.08593*, 2019.
- 622
 623
 624
 625
 626
 627
 628
 629
 630
 631
 632
 633
 634
 635
 636
 637
 638
 639
 640
 641
 642
 643
 644
 645
 646
 647